Small-Scale Features in the ΔfCO_2 Distributions Along the TN413 Cruise Track in the North Pacific Subtropical Gyre and Equatorial Pacific

Jace Marquardt

University of Washington

School of Oceanography, Box 357940

Seattle, WA 98195-7940

Email: jacem26@uw.edu

June 2, 2023

Abstract

Rising atmospheric CO_2 levels are contributing to widespread changes in the global ocean carbon budget. Long-term trends on the air-sea flux of CO_2 have demonstrated that the North Pacific Subtropical Gyre (NPSTG) is a net sink of CO_2, whereas the equator is a net source. There are sparse smaller spatial and temporal scale analyses of ΔfCO_2 features in the Pacific Ocean; this study aimed to resolve this by collecting underway fCO_2, SSS, SST, and phytoplankton abundance data from cruise TN413 from February 24—March 12, 2023. It was hypothesized that ΔfCO_2 levels would be similar to previous data—lower in the gyre and higher in the equatorial region. In addition, horizontal gradients in ΔfCO_2 in the NPSTG would be a result of biological processes rather than physical because of its highly stratified water. ΔfCO_2 features in the equatorial Pacific would be driven by physical processes due to upwelling bringing old, CO_2-supersaturated water to the surface. Current ΔfCO_2 data matched previous data from March 2000, however there were two areas in the NPSTG where significant horizontal gradients were present (6°N and 10°N). Because of the anticorrelation between ΔfCO_2 and SST at 6°N, upwelling is thought to have transported nutrients, influencing primary productivity, and decreasing fCO_2 by photosynthesis. The gradient at 10°N had positive correlations with SSS and SST, so it was probably caused by equatorial water that was transported by a tropical instability wave or an eddy. Further research is needed to confidently identify the source of the feature at 10°N.

Plain Language Summary

Rising atmospheric CO_2 levels cause widespread changes in the CO_2 levels in the ocean. Studies on the exchange between the atmosphere and ocean have found that the North Pacific Subtropical Gyre typically absorbs CO_2 from the air, whereas the equator releases CO_2. There is a lack of research on how the difference in atmosphere and ocean CO_2 levels changes across smaller regions. This study aimed to resolve this by using sea surface CO_2, temperature, salinity, and phytoplankton data from research cruise TN413 to analyze why there are changes in CO_2 over small regions of the ocean. It was thought that CO_2 levels would be similar to previous findings—lower in the gyre and higher at the equator. Moreover, areas of increased CO_2 in the gyre should be caused by biological activity rather than the physical movement of water because the gyre typically does not experience mixing between the deep ocean and surface. However, CO_2 changes at the equator should be caused by physical processes because of the deep water mixing that occurs. CO_2 data from 2023 matched previous data, however there were two areas where changes in CO_2 were present (6°N and 10°N). Because of the opposite relationship between CO_2 and temperature at 6°N, upwelling might have transported nutrients upward which increased biological activity, decreasing CO_2 levels by photosynthesis. The change in CO_2 at 10°N was positively related to salinity and temperature, so it was probably caused by equatorial water carried by currents diverging north.

Introduction

Carbon Dioxide in the Ocean

Ever since the Industrial Revolution, atmospheric CO_2 concentrations have been rising rapidly. Carbon dioxide is not static, however. It transfers between the atmosphere and oceanic and terrestrial sources and sinks. Decades of research has shown that atmospheric CO_2 concentrations continue to grow because of anthropogenic emissions (e.g., Marland & Rotty, 1984; Boden et al., 2009). With an abundance of research showing the potential hazards of increasing CO_2 in the atmosphere leading to climate-related impacts, it becomes ever more important to understand how the sources and sinks of CO_2 are functioning. To better predict the severity of the impacts of climate change, we must increase our knowledge of how CO_2 interacts with the ocean. Areas like the Southern Ocean, for example, are sinks for carbon dioxide, whereas areas like the Equator are typically sources (e.g., Gruber et al., 2009). The ocean is a major exchanger of carbon reservoirs, effectively controlling the atmospheric concentration of carbon dioxide (Siegenthaler & Wenk, 1984). The global oceans absorb around 25% of the anthropogenic CO_2 from the atmosphere every year (Sabine et al., 2004; Takahashi et al., 2009). Anthropogenic carbon dioxide controls the majority of the pCO_2 trends in the ocean, with 40% being driven by natural variability, such as Pacific Decadal Oscillation, in which there are widespread variations in temperature in the surface water of the Pacific Ocean (Sutton et al., 2014).

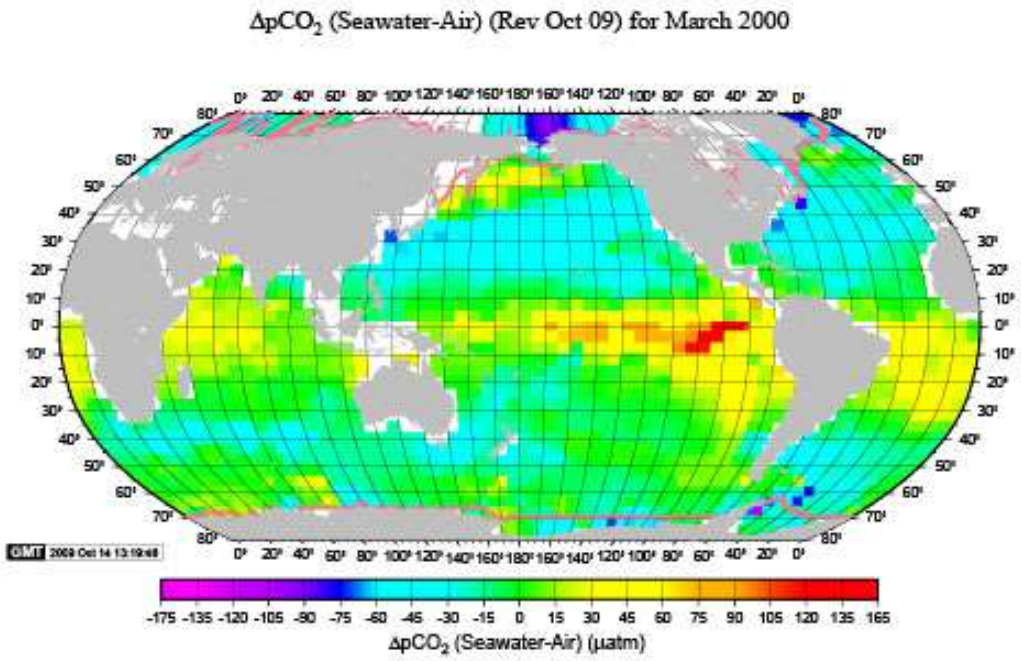

Figure 1. Map of ΔpCO_2 concentration (µatm) across the global ocean for March 2000. The equatorial region is the largest source of carbon dioxide to the atmosphere ($\Delta pCO_2 > 0$), whereas the North Pacific Subtropical gyre is a sink for CO_2 ($\Delta pCO_2 < 0$). Figure from Takahashi et al. (2009).

Equatorial Pacific

The equatorial Pacific is the largest oceanic source of CO_2 to the atmosphere (Pittman et al., 2022; Takahashi et al., 2009; Figure 1). El Niño-Southern Oscillation (ENSO) events are the main drivers for interannual variability of the surface water pCO_2 in this region (Rayner & Law, 1999; Sutton et al., 2014). Water upwelled at the equator has been shown to be recycled surface water or entrained water from the subtropical Pacific regions (McCreary & Lu, 1994; McPhaden & Zhang, 2002). During La Niña events, carbon export out of the equatorial region is greater than El Niño events due to upwelling of older water that is supersaturated in CO_2 (Barber et al., 1994; Sutton et al., 2014). Large seasonal pCO_2 variation can occur in the equatorial "cold

tongue" region because of variable upwelling during La Niña events (Yasunaka et al., 2019). Variation can also be attributed to a warming ocean, which results in a reduction of carbon uptake (McKinley et al., 2011). When water becomes warmer, its gas solubility decreases. Therefore, as anthropogenic climate change continues to increase water temperatures, the role the ocean plays in the global carbon cycle is bound to change. Warming sea surface temperatures, weaker trade winds, and shoaling of the thermocline are predicted by models to cause the equatorial Pacific to become an even greater source of CO_2 to the atmosphere in the future (Vaittinada Ayar et al., 2022).

North Pacific Subtropical Gyre

The North Pacific Subtropical Gyre (NPSTG) tends to be a net sink of carbon dioxide (Figure 1). Only during extreme El Niño events, where surface temperatures in the Pacific Ocean are anomalously high, does the gyre become a source of CO_2 to the atmosphere (Sutton et al., 2017). Surface seawater pCO_2 concentration has been increasing in the gyre over time, along with warm temperature anomalies intensifying (Sutton et al., 2017). Moreover, the rate of pCO_2 increase is also expected to rise from seawater equilibrium with the escalating atmospheric carbon dioxide concentrations (Sutton et al., 2017). Like ENSO in the equatorial region, the NPSTG experiences climate variability called the North Pacific Gyre Oscillation. This oscillation is correlated with fluctuations in salinity, nutrients, and chlorophyll in the gyre (Lorenzo et al., 2008). Wind-driven upwelling and horizontal advection bring nutrients to the surface, allowing for more primary production during such oscillations or La Niña events.

Sea Surface Temperature and Salinity

Seawater pCO_2 concentrations have been strongly correlated with sea surface temperature (SST) (Chen et al., 2007; Sutton et al., 2017). In the NPSTG, surface pCO_2 is primarily controlled by thermodynamics, and thus has a positive relationship (Chen et al., 2007). When a cold-core cyclonic eddy is present, a negative relationship is observed as a result of the upwelling of CO_2-rich subsurface waters, biological uptake, and changes in temperature and salinity (Chen et al., 2007). Such eddies are formed by a diverging warmer water current wrapping around a colder water mass. A gradient in the isopycnals of each water mass is converted into kinetic energy in the form of flow around the eddy. This could result in upwelling in the center of the eddy, represented by a decrease in temperature and increase in nutrients. In the equatorial Pacific, SST and pCO_2 are inversely correlated (Sutton et al., 2014). The anticorrelation of these in the equatorial Pacific is caused by the strong influence of upwelled DIC-rich water in surface pCO_2 concentration (Sutton et al., 2014).

Sea surface salinity (SSS) has also been weakly correlated with surface pCO_2; however, strong upper ocean physical mixing increases the correlation between these two (Sutton et al., 2017). Significantly changing trends in SSS are less of an indicator of pCO_2 changes and more of an indicator of larger biogeochemical processes happening in a region.

Biological Productivity

When looking at long-term seawater pCO_2 trends in the equatorial Pacific, variations of pCO_2 can be attributed to changes in biological production (Sutton et al., 2014). Upwelling has been found to be the main source of changes in biological production in the equatorial region due to the deliverance of limited nutrients (Coale et al., 1996). The equatorial Pacific tends to be a

high nutrient-low chlorophyll (HNLC) region most likely limited by iron or silica (Dugdale & Wilkerson, 1998). When there is a rise in biological production, there is a subsequent decrease in pCO_2 because of the increased rate of photosynthesis utilizing carbon dioxide in the water. However, increasing SST has been found to decrease new primary production despite an overall increase in dissolved inorganic carbon in the equatorial region (Pittman et al., 2022). Therefore, regardless of upwelling at the equator, there could still be low primary production due to unfavorable high-temperature conditions.

It has been suggested that phytoplankton blooms in the NPSTG are not due to changes in the subsurface structure like upwelling, but rather are caused by biological processes such as nitrogen fixation or vertical migration of zooplankton delivering nutrients to the surface (Wilson, 2003). The NPSTG is dominated by large mesoscale anticyclonic circulation that is characterized by oligotrophic conditions and low pCO_2, although short bursts of nutrients can be delivered to the NPSTG by vigorous vertical upwelling caused by wind-driven currents and small-scale cyclonic eddies (Lee et al., 1994; Karl, 1999). These bursts of primary production produce high rates of respiration, but subsequently lower pCO_2 concentrations in the surface water. Alternatively, primary production in the gyre can be initiated by nitrogen fixation. N_2 fixation has been found to account for nearly half of the NPSTG's nitrogen budget (Karl et al., 1997). An increase in production initiated by nitrogen fixation would result in a similar chemical state as eddies, with high photosynthetic production and low pCO_2. If nitrogen fixation were occurring, SST and SSS would remain unchanged due to little to no vertical mixing, while eddies and wind-driven currents would cause a change in these properties.

Hypothesis

Several long-term studies of ΔpCO_2 have been conducted over the years, however there is a lack of high-resolution data across small spatial and temporal scales in the Pacific Ocean (Takahashi et al., 2009; Qui et al., 2021). Much of the previous literature on carbon dioxide in the Pacific used fixed moorings to collect ΔpCO_2 data, which is averaged weekly or monthly, or is in a gridded form that does not allow for a resolution of spatial scales smaller than ~4° latitude (e. g., Sutton et al., 2014, 2017; Takahashi et al., 2019). With climate change continuing to impact our global oceans, it is important to gather more recent data to improve climate models. Currently, climate change carbon cycle models for the equatorial Pacific are uncertain, lacking seawater pCO_2 data (Sutton et al., 2014). There have been experiments with using satellite-based data to estimate pCO_2 in the North Pacific, but there is a lack of in situ shipboard data that could help refine the estimating equations (Sarma et al., 2006). This study aims to resolve the smaller spatial scale variations of ΔpCO_2 in the Pacific Ocean by using real-time underway pCO_2 data. Instead of using partial pressure, however, this study will use fugacity to determine CO_2 concentrations. This is because fugacity accounts for the non-ideal behaviors that carbon dioxide exhibits and is considered a more accurate representation of the true gas concentration. So, ΔfCO_2 will be the focus of this study rather than ΔpCO_2.

It is hypothesized that the results of this study will align with previous research conducted on ΔpCO_2 in the NPSTG and equatorial Pacific, with higher ΔfCO_2 levels in the equatorial region and lower levels in the gyre. ΔfCO_2 should be steady in the NPSTG, then increase rapidly in the equatorial Pacific due to regional upwelling delivering CO_2-enriched water to the surface. There should be small-scale spatial features in ΔfCO_2 concentration where it increases or decreases due to local physical and biological processes that act on daily or weekly

timescales. Significant features in ΔfCO_2 at the equator are more likely to be a result of physical processes rather than biological because of the strong correlation between upwelling bringing CO_2 supersaturated water to the surface. In the NPSTG, it is predicted that significant features observed by rapid changes in ΔfCO_2 will be driven by biological processes such as blooms caused by nitrogen fixation because of the lack of vertical mixing that occurs in the NPSTG. We also expect to see minimal changes in ΔfCO_2 in the NPSTG because of the lack of mixing and homogenously low biomass present under normal conditions.

Methods

Data were collected during the University of Washington senior thesis research cruise TN413 aboard the R/V Thomas G. Thompson. The ship departed from Honolulu, HI, on February 24, 2023, and began sampling a meridional section across the equator on March 4, 2023, from 5°N to 5°S along 180°, stopping at 15 stations for conductivity, temperature, and depth (CTD) sampling (Figure 2). After the meridional section, the R/V Thompson transited to Suva, FJ, and arrived on March 12, 2023.

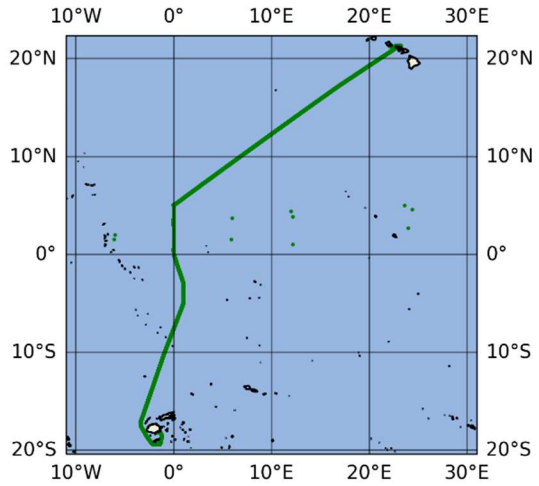

Figure 2. Map of research cruise TN413 on the R/V Thomas G. Thompson from February 24 to March 11, 2023. TN413 departed from Honolulu, HI and docked in Suva, FJ.

Surface seawater pCO_2, atmospheric pCO_2, SST, and SSS were collected along the entire cruise transect. The ship's seawater intake system on the R/V Thompson provided continuous flow of seawater collected at an estimated depth of 5 m. Seawater pCO_2 was measured using the underway pCO_2 system described in Pierrot et al. (2009), which was attached to the seawater intake system (Figure 3). Atmospheric pCO_2 was measured on the bow of the vessel at an estimated height of 10 m above sea level. It is designed to be accurate to within 0.1 µatm for atmospheric measurements and within 2 µatm for seawater measurements. SST and SSS were measured using the collected seawater and sampled with a thermosalinograph integrated into the intake system. There was missing data from 8°S to Suva, FJ, because communications between the pCO_2 instrument and the R/V Thompson's thermosalinograph and navigation system had a glitch and resulted in corrupted data.

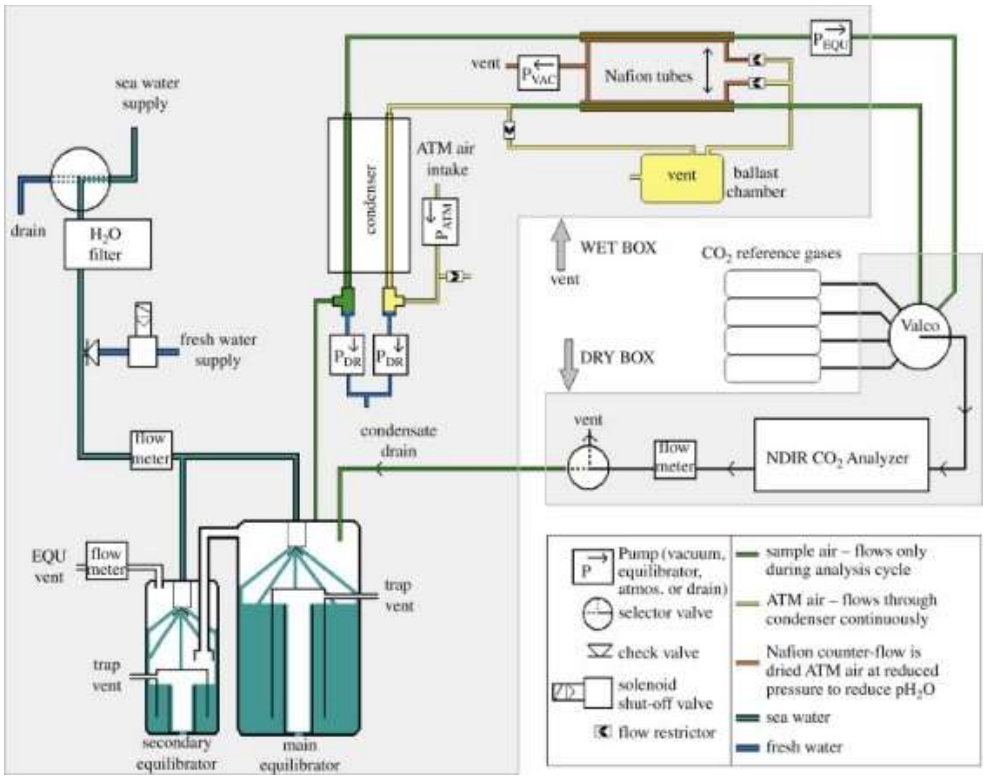

Figure 3. Shipboard pCO_2 intake system on the R/V Thomas G. Thompson (Pierrot et al., 2009).

Fugacity is used to account for the non-ideal behaviors of gases and can be considered a more accurate calculation for carbon dioxide concentrations since CO_2 is a non-ideal gas. ΔfCO_2 uses fugacity rather than partial pressure to measure the difference between oceanic and atmospheric carbon dioxide. Post-processing of the pCO_2 data collected was done by the NOAA Pacific Marine Environmental Laboratory to calculate fCO_2. ΔfCO_2 was then calculated by taking the difference between seawater fCO_2 and atmospheric fCO_2:

$$\Delta fCO_2 = fCO_{2sw} - fCO_{2air} \quad (1)$$

Surface pCO_2 data for March 2000 from the Global Surface pCO_2 (LDEO) Database V2019 was used as reference to compare previous pCO_2 data to data collected by TN413 (Takahashi et al., 2019). The LDEO dataset is comprised of approximately 14.2 million measurements of surface pCO_2 made during 1957-2019 and were compiled and gridded with a spatial resolution of 4° latitude x 5° longitude. The global LDEO pCO_2 data is available at: https://www.nodc.noaa.gov/ocads/oceans/LDEO_Underway_Database/. The portion of the data used in this study was during the time March 2000 between 22°N to 10°S and 157°W to 180°W. Oceanic Niño Index (ONI) data were provided by the NOAA / National Weather Service (NWS) Climate Prediction Center at: https://origin.cpc.ncep.noaa.gov/products/analysis_monitoring/ensostuff/ONI_v5.php (accessed on May 13, 2023). The ONI is determined by applying a 3 month running mean of ERSSTv5 SST anomaly data from 5°N to 5°S and 120°W to 170°W (Huang et al., 2017). El Niño events are represented by ONI values > 0.5, La Niña events are < -0.5, and neutral conditions are between -0.5 and 0.5.

To observe biological productivity in the water, a custom-built shipboard flow cytometer called SeaFlow was used (Swalwell et al., 2011). The water collected by the ship seawater intake

was run through SeaFlow and measured the abundance of picoeukaryotes (0.2 - 3 μm in diameter). SeaFlow measured both scatter and chlorophyll concentrations to calculate the population abundance of these phytoplankton. SeaFlow then differentiated between *Synechococcus* (1-2 μm in diameter), *Prochlorococcus* (<1 μm in diameter), and other phytoplankton present designated as picoeukaryotes. These plankton were useful to sample because *Synechococcus* has the enzyme nitrogenase, allowing them to fix nitrogen, while *Prochlorococcus* is understood to not be able to fix nitrogen.

All data analysis was completed with Python in a Jupyter notebook. Plotting was done using the Matplotlib and Cartopy packages, and calculations were done with the Pandas and SciPy packages.

Results

Carbon Dioxide

In the NPSTG, ΔfCO_2 remained negative, with values ranging between 0 μatm and -40 μatm (Figure 4A). There were small features in ΔfCO_2 across latitude in this region, including from 10°N to 12°N and 6°N to 7°N. Around 6-7°N, there was a strong horizontal gradient in ΔfCO_2 from 1.53 μatm to 44.77 μatm that took place within ~1-2° latitude (Figure 4A). Similarly, at 4°N ΔfCO_2 quickly increased in value as the ship crossed into the equatorial region from 25.7

µatm to 71.8 µatm (Figure 4A). ΔfCO_2 concentration peaked at 101 µatm at the equator, and began to decrease again at 4°S.

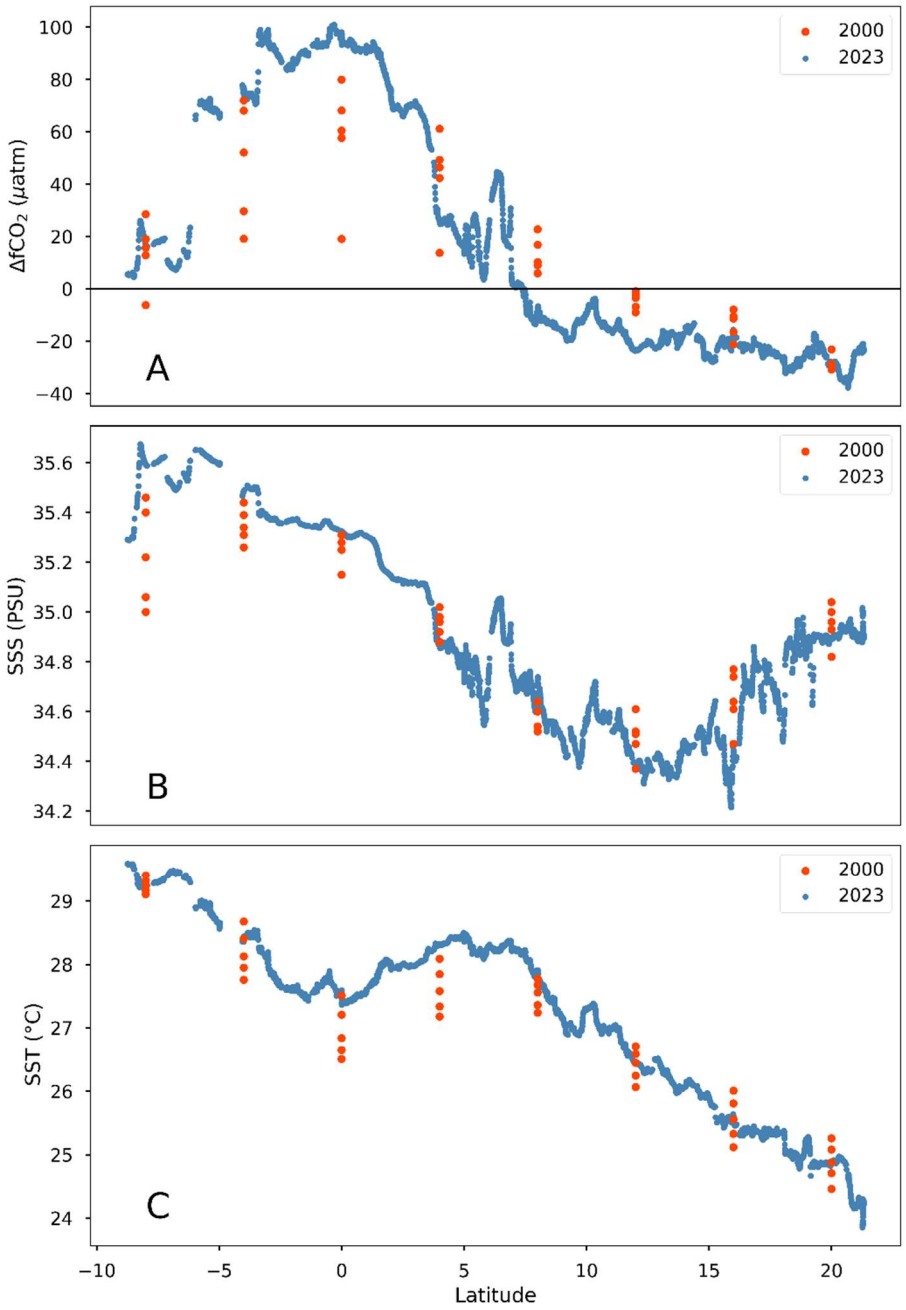

Figure 4. Graph of ΔfCO_2 (A), SSS (B), and SST (C) from March 2000 (red) and March 2023 (blue). The horizontal black line on Graph A represents where the atmospheric fCO_2 and oceanic fCO_2 are equal in value. Generally, the trends are the same for 2000 and 2023, but there are smaller spatial scale changes in values revealed in 2023 compared to the binned 2000 data (Takahashi et al., 2009).

In comparison with the mean ΔpCO_2 concentrations for March 2000 presented by Takahashi et al. (2009), ΔfCO_2 was higher in the equatorial region in 2023 (Figure 4A). Furthermore, the southern extent of negative ΔfCO_2 values shifted from around 12°N in 2000 to 7°N in 2023. ΔfCO_2 concentration near 6°N nearly doubled compared to March 2000 (Figure 4A). The peak ΔfCO_2 concentration at the equator was also higher in 2023, increasing by 21.04 µatm above the 2000 data.

March 2000 Comparison

Overall, ΔfCO_2, SSS, and SST collected on research cruise TN413 followed very similar trends to the mean March 2000 data compiled by Takahashi et al. (2009). From around 8°N to 20°N ΔfCO_2 was negative in value, and from 8°N to 8°S it was positive (Figure 4A). Moreover, SSS and SST also had similar trends across latitude compared to their equivalent 2000 data. Salinity reached a minimum value of 34.215 PSU around 12°N to 16°N in both 2000 and 2023 (Figure 4B). It then reached a peak value of 35.675 PSU in 2023 and 35.460 PSU in 2000 around 9°S. SST was nearly identical to the mean March 2000 data as well. SST gradually increased to 5°N, then decreases around the equator, and increased to a peak of ~30 °C at 9°S (Figure 4C). The Oceanic Niño Index (ONI) was -1.1 in March 2000 and -0.2 in March 2023 (Table 1).

Table 1. Oceanic Niño Index from 1999-2000 and 2022-2023. Columns are indicated by 3-month means. Larger negative numbers represent stronger La Niña conditions. Data provided by NOAA/NWS Climate Prediction Center.

Year	DJF	JFM	FMA	MAM	AMJ	MJJ	JJA	JAS	ASO	SON	OND	NDJ
1999	-1.5	-1.3	-1.1	-1.0	-1.0	-1.0	-1.1	-1.1	-1.2	-1.3	-1.5	-1.7
2000	-1.7	-1.4	-1.1	-0.8	-0.7	-0.6	-0.6	-0.5	-0.5	-0.6	-0.7	-0.7
2022	-1.0	-0.9	-1.0	-1.1	-1.0	-0.9	-0.8	-0.9	-1.0	-1.0	-0.9	-0.8
2023	-0.7	-0.4	-0.2									

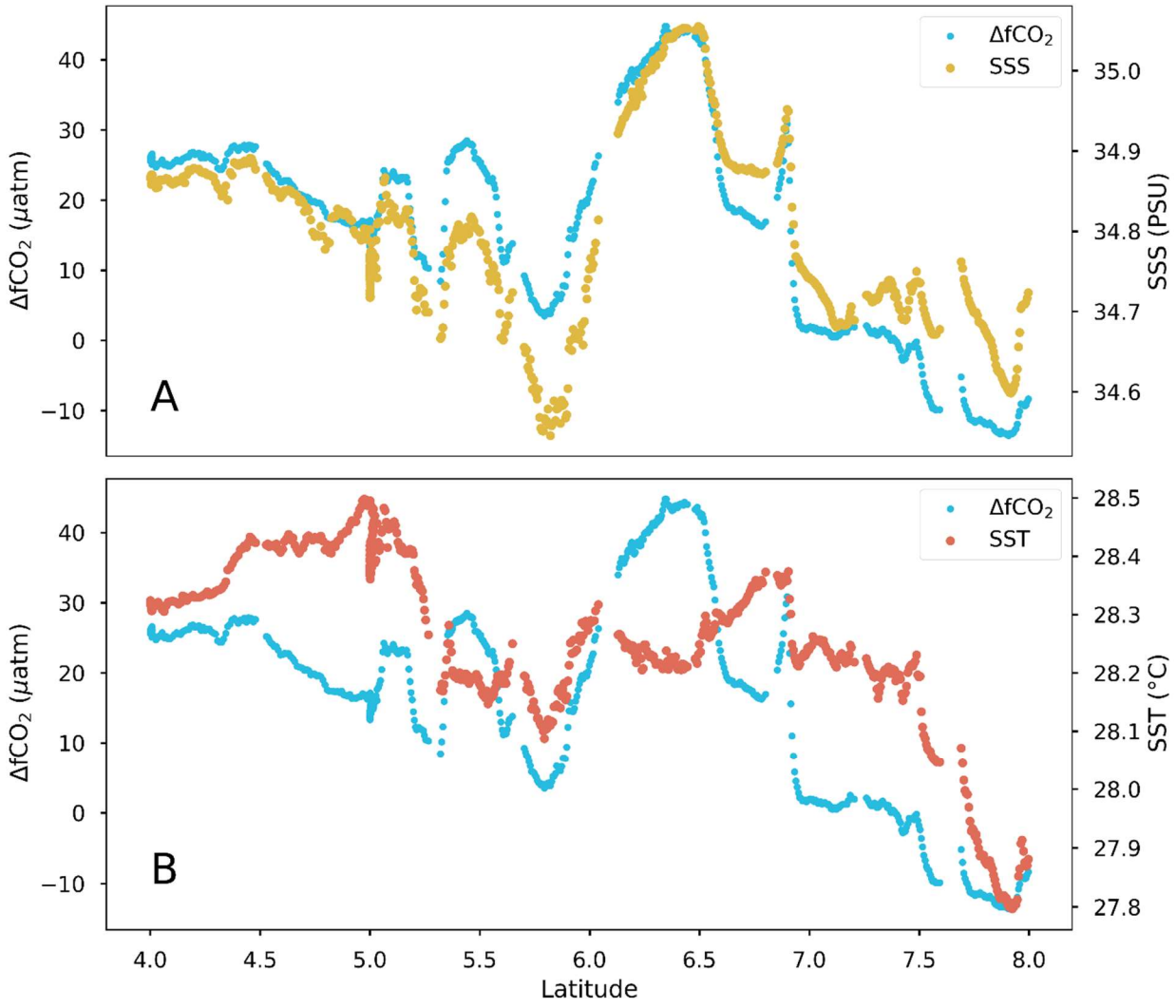

Figure 5. Plots of ΔfCO_2—cyan (A/B), SSS—yellow (A), and SST—red (B) from 4°N to 8°N.

Sea Surface Salinity

In the same region as the strong horizontal gradient in ΔfCO_2 from 6-7°N, salinity displayed a similar trend (Figure 5A). The salinity concentration changed by 0.678 PSU between 6°N and 10°N. At ~4°N, there was another rapid increase in salinity (Figure 4B). Salinity reached its peak concentration of 35.675 PSU at ~8°S. Compared to ΔfCO_2, an r^2 value of 0.5868 suggests that salinity did not have a strong correlation with ΔfCO_2 over the whole cruise transect, however

there was minor correlation from 4°N to 8°N where $r^2 = 0.7207$ (Figure 6).

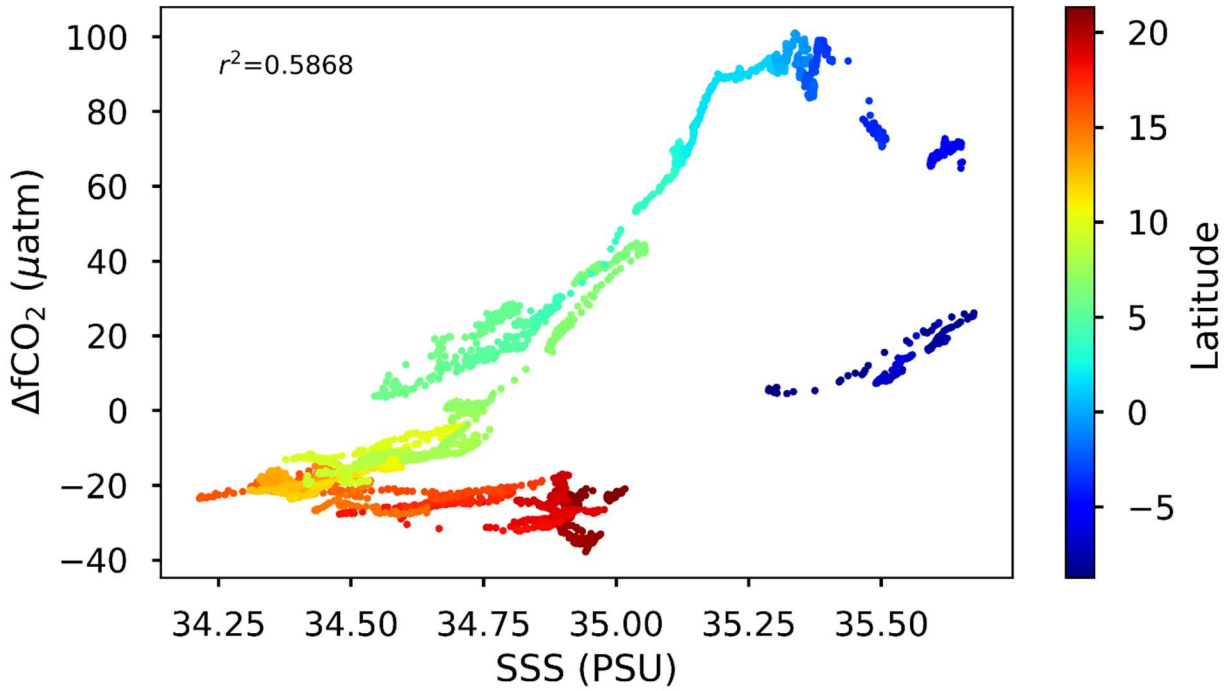

Figure 6. Correlation graph between ΔfCO$_2$ (μatm) and SSS (PSU). The points on the graph are colored by latitude, with red being 20°N and blue being 5°S.

Sea Surface Temperature

SST followed different trends than ΔfCO$_2$ and salinity. Sea surface temperatures slowly rose with decreasing latitude to 28.498 °C at ~5°N (Figure 4C). From there, SST decreased to the lowest temperature recorded in the equatorial region at around 0° (Figure 4C). Like salinity, the peak SST was recorded south of the equator at ~8°S with a temperature of 29.607 °C. Sea surface temperature did not have any strong horizontal gradients across latitude. Overall, SST did not have a strong correlation to ΔfCO$_2$ concentration (Figure 7). However, an inverse relationship was present in the equatorial region, with ΔfCO$_2$ increasing while SST decreased (Figure 4).

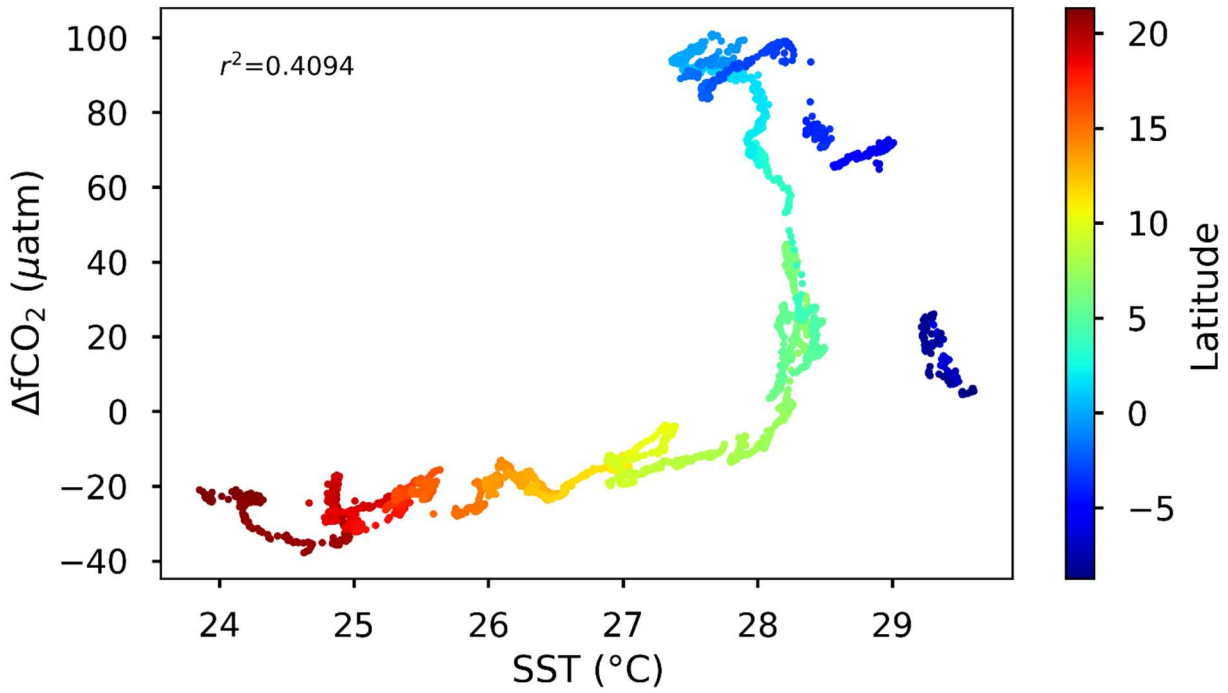

Figure 7. Correlation graph between ΔfCO₂ (μatm) and SST (°C). The points on the graph are colored by latitude, with red being 20°N and blue being 5°S.

Phytoplankton Abundance

Picoeukaryote and *Synechococcus* abundance remained low (~10 cells/μL; ~2 cells/μL) within the gyre until a large increase in abundance occurred around 12°N (Figure 8). Picoeukaryote abundance increased to ~43 cells/μL and *Synechococcus* increased to ~25 cells/μL within 2° latitude. *Prochlorococcus* was more abundant than picoeukaryotes and *Synechococcus*, but it displayed a strong horizontal gradient in abundance as well, increasing by ~129 cells/μL (Figure 8). From 6°N to 9°N, there was another rapid horizontal gradient in plankton abundance, with all three types of picoplankton increasing dramatically (Figure 8). *Synechococcus* increases from 0.7 cells/μL at 9°N and ends at 49 cells/μL at ~7.5°N (Figure 8). The picoeukaryotes were

in their highest abundance at ~6°N with a peak concentration of 54 cells/µL (Figure 8). Similarly, *Prochlorococcus* reached a peak at 235 cells/µL at 6°N (Figure 8).

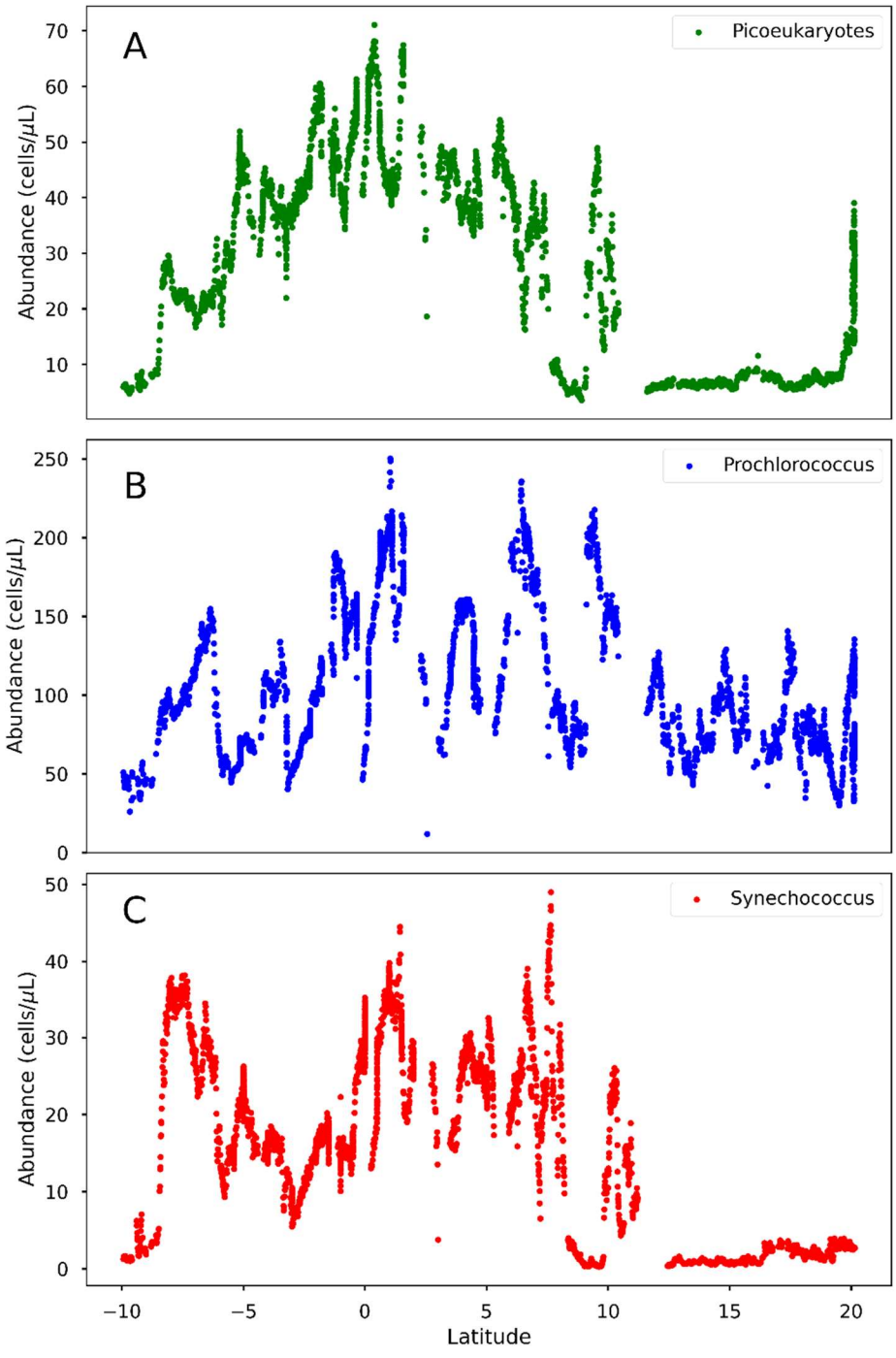

Figure 8. Plots of picoeukaryote (A), Prochlorococcus *(B), and* Synechococcus *(C) abundance from SeaFlow data on cruise TN413. All three groups experienced an increase in abundance at 6°N and 10°N.*

Discussion

The ΔfCO_2 data collected by TN413 resembled March 2000 data presented by Takahashi et al. (2009), with higher ΔfCO_2 values in the equatorial Pacific and lower in the NPSTG. There were two locations at the gyre in which there were strong horizontal features in ΔfCO_2. From 6°N to 7°N, ΔfCO_2 was positively correlated with SSS, inversely correlated with SST, and positively correlated with phytoplankton abundance. This suggests that the increase in ΔfCO_2 in this region was likely caused by regional upwelling bringing CO_2-enriched water to the surface, along with nutrients to drive primary production. Similarly, from 10°N to 12°N there was also a significant ΔfCO_2 feature. Unlike 6°N to 7°N, however, ΔfCO_2 was positively correlated with all the parameters examined including SST. Warm, salty water from the equator could have been transported to the gyre in the form of a TIW or cyclonic eddy and carried water supersaturated in CO_2 and nutrients. The physical transport of water from the equatorial region would explain why there is an increase in SST with ΔfCO_2. Therefore, both regions in the NPSTG where ΔfCO_2 features increased rapidly are likely due to physical processes rather than biological.

It is surprising that the equatorial ΔfCO_2 data collected in 2023 were greater in value than in 2000 given that the ONI indicated a La Niña phase in 2000 and neutral conditions in 2023 (Table 1). Equatorial upwelling should have been stronger in 2000 because of the La Niña conditions, so theoretically there should have been higher ΔfCO_2 values. Interestingly, this was not the case. One possible explanation for this is that the cruise in 2023 occurred at the end of a third consecutive La Niña event. It is reasonable that ΔfCO_2 would be higher because there was increased equatorial upwelling in the past three years accumulating CO_2 at the surface (Sutton et al., 2017). The March 2000 data were collected in the middle of a second consecutive La Niña event, not a third like in 2023, so there should be less surface pCO_2 observed. It is also possible

that there was stronger local upwelling on a smaller timescale, on that of days rather than weeks. TN413 could have passed through the equatorial region during a time of greater vertical upwelling.

Unlike the data presented by Takahashi et al. (2009) and Sutton et al. (2017), the data collected by TN413 revealed small-scale spatial changes in ΔfCO_2. This was to be expected, given that their data was binned or moored and averaged monthly. Around 6°N to 7°N, there was a strong horizontal gradient feature in ΔfCO_2 in 2023 that was not apparent in the data from 2000 (Figure 4). Due to the strong relationship between SSS and ΔfCO_2 and slight decrease in SST, it is probable that regional upwelling occurred. Picoeukaryote, *Prochlorococcus*, and *Synechococcus* abundance all increased dramatically in this region. The upwelled water likely delivered limited nutrients like iron or silica from the deep ocean to drive biological productivity and surfaced old water rich in CO_2 increasing the ΔfCO_2 values. If a biological source like nitrogen fixation were the dominating feature in this area, then a correlation with *Synechococcus* would have been present and ΔfCO_2 would have decreased in value because of photosynthetic activity. Therefore, the change in ΔfCO_2 at 6°N to 7°N was most likely caused by physical upwelling rather than biological processes.

A less intense feature of ΔfCO_2 was observed from 10°N to 12°N (Figure 4). SSS and SST increased there, too. Even though this horizontal gradient in ΔfCO_2, SSS, and SST was less than at 6°N, there was an equally strong increase in phytoplankton abundance (Figure 8). Since the equator had a high salinity and high ΔfCO_2, it appears that the gradient might have been created by a tropical instability wave (TIW) or drifting cyclonic eddy from the equator that transported surface water that was higher in CO_2 northward to the gyre. A TIW or eddy would explain the rapid increase and rapid decrease in ΔfCO_2 because TIW's and cold-core eddies are

characterized by one body of water wrapping around another. So, equatorial water—warm and higher in CO_2—could have been wrapped around colder, low-CO_2 water from the NPSTG. It is also possible that this strong horizontal gradient in ΔfCO_2 was created by surface currents from the western Pacific shifting eastward. During receding La Niña conditions, the equatorial currents shift from westward movement to eastward. CO_2 supersaturated water from equatorial upwelling was possibly driven to the west Pacific by La Niña surface currents, then transported east by the shifting ENSO phase resulting a change in direction of currents and observed by TN413 as a strong horizontal gradient feature in ΔfCO_2. It is important to note, though, that phytoplankton communities are known to be resilient on timescales of days to weeks after physical forcings in the NPSTG (Rii et al., 2022). Therefore, there could have been strong vertical mixing in this region before TN413 collected the data, explaining why there is a less strong signal in ΔfCO_2, SSS, and SST while maintaining high phytoplankton abundance. This would also make sense given that approximately 10°N is where the Northern Equatorial Countercurrent (NECC) lies, which has been shown to have a reversal in current direction and results in vertical Ekman pumping to the surface (Kessler, 2006). So, it is surprising that there was an increase in SST observed during the 2023 sampling rather than a decrease.

For most of the cruise transect, ΔfCO_2 was not strongly correlated with SSS. This is supported by previous findings that salinity is not directly related to ΔfCO_2 concentration (Sutton et al., 2017). However, from 6°N to 7°N and 10°N to 12°N ΔfCO_2 and SSS were positively correlated, with both concentrations increasing rapidly in a small region (Figure 4). Sutton et al. (2017) found that when SSS and pCO_2 are strongly correlated, it is likely not a cause-and-effect relationship between the two, but rather an indication of larger biogeochemical processes

happening. This supports the idea that the intense horizontal gradient in ΔfCO_2 and SSS observed at 6°N to 7°N and 10°N to 12°N were a result of physical oceanic processes.

Interestingly, there was overall no significant correlation with ΔfCO_2 and SST along the cruise transect. Although, as hypothesized when TN413 crossed the equatorial region, there was an inverse relationship between ΔfCO_2 and SST, supporting the conclusion that there is an inverse relationship at the equator (Sutton et al., 2014). The inverse relationship is due to equatorial upwelling of old water that is cold and supersaturated in CO_2. On the other hand, the hypothesis that there would be a positive correlation between SST and ΔfCO_2 in the NPSTG was not supported. This is contrary to previous research which had found that pCO_2 is positively correlated with SST in the gyre (Sutton et al., 2017). Without further investigation of surface currents and wind patterns, it is unknown why there was no significant correlation between ΔfCO_2 and SST in the gyre.

Though, it must be acknowledged that the data collected from 2023 were instantaneous samples and take that into consideration when forming hypothesis for why the observed trends occur. Instantaneous samples are subject to variability on very short timescales (e.g., hours, days) that could produce inaccurate results for analyzing oceanic processes that operate on longer timescales (e.g., weeks, months). Consequently, the samples from 2023 might not be a complete and accurate representation of the general trends in the NPSTG and equatorial Pacific. In addition, the SeaFlow data was consistently taken during the cruise, so the phytoplankton population abundances seen at the surface could have been affected by daily processes, resulting in a diurnal trend. Thus, the primary production trends assumed by the population abundance could also be inaccurate for assessing general primary production trends along the TN413 cruise track.

Conclusions

As anthropogenic carbon dioxide continues to be emitted at greater rates, it will be important to monitor how the global ocean carbon cycle is impacted. Studying how the various sinks and sources of CO_2 are affected will help us understand how natural variability impacts small-scale spatial and temporal features in the surface ocean. This research looked at ΔfCO_2 along the TN413 cruise track and found that the local features where there are significant horizontal gradients in ΔfCO_2 at 6°N-7°N and 10°N-12°N were caused by physical processes. There was also no significant correlation between SST and ΔfCO_2 which is different from previous findings. There were significant correlations between SSS and ΔfCO_2 at 6°N-7°N indicating larger biogeochemical processes occurring such as regional upwelling.

Further investigation on nutrient concentrations would be beneficial to confirm that these regions of high biological productivity are from an increase in nutrients delivered by physical processes. It would also be helpful to measure surface current direction, as well, to observe if any eddies or TIW's were present. It is possible that from 6°N to 7°N water was transported from the west Pacific, so measuring current direction could determine the validity of this hypothesis. Moreover, SST did not have significant correlations with ΔfCO_2. This is the opposite of what previous literature has determined, so more data from the study region would be useful.

Acknowledgements

First, I would like to thank my mentor Mark Warner for his guidance throughout the research process. I also want to thank all the other professors in OCEAN 445 who have provided their moral and intellectual support. Special thanks to Kelsey Cain and Francois Ribalet for

operating SeaFlow, and to all the crew aboard the R/V Thomas G. Thompson. I also want to acknowledge the financial support provided by the University of Washington School of Oceanography which allowed me to collect much of the data personally and has given me an amazing experience and education as an oceanography student.

References

Barber, R. T., Murray, J. W., & McCarthy, J. J. (1994). Biogeochemical interactions in the equatorial Pacific. *Ambio (Journal of the Human Environment, Research and Management)*, *23*(1), 62–66.

Boden, T. A., Marland, G., & Andres, R. J. (2009). Global, regional, and national fossil-fuel CO2 emissions. *Carbon Dioxide Information Analysis Center, Oak Ridge National Laboratory, US Department of Energy, Oak Ridge, Tenn., USA*, *10*.

Chen, F., Cai, W.-J., Benitez-Nelson, C., & Wang, Y. (2007). Sea surface pCO2-SST relationships across a cold-core cyclonic eddy: Implications for understanding regional variability and air-sea gas exchange. *Geophysical Research Letters*, *34*(10). https://doi.org/10.1029/2006GL028058

Coale, K. H., Fitzwater, S. E., Gordon, R. M., Johnson, K. S., & Barber, R. T. (1996). Control of community growth and export production by upwelled iron in the equatorial Pacific Ocean. *Nature*, *379*, 621–624. https://doi.org/10.1038/379621a0

Dugdale, R. C., & Wilkerson, F. P. (1998). Silicate regulation of new production in the equatorial Pacific upwelling. *Nature*, *391*, 270–273. https://doi.org/10.1038/34630

Gruber, N., Gloor, M., Mikaloff Fletcher, S. E., Doney, S. C., Dutkiewicz, S., Follows, M. J., Gerber, M., Jacobson, A. R., Joos, F., Lindsay, K., Menemenlis, D., Mouchet, A., Müller,

S. A., Sarmiento, J. L., & Takahashi, T. (2009). Oceanic sources, sinks, and transport of atmospheric CO2. *Global Biogeochemical Cycles*, *23*(GB1005). https://doi.org/10.1029/2008GB003349

Huang, B., Thorne, P. W., Banzon, V. F., Boyer, T., Chepurin, G., Lawrimore, J. H., Menne, M. J., Smith, T. M., Vose, R. S., & Zhang, H.-M. (2017). Extended reconstructed sea surface temperature, version 5 (ERSSTv5): Upgrades, validations, and intercomparisons. *Journal of Climate*, *30*(20), 8179–8205.

Karl, D., Letelier, R., Tupas, L., Dore, J., Christian, J., & Hebel, D. (1997). The role of nitrogen fixation in biogeochemical cycling in the subtropical North Pacific Ocean. *Nature*, *388*(6642), 533–538. https://doi.org/10.1038/41474

Karl, D. M. (1999). A Sea of Change: Biogeochemical Variability in the North Pacific Subtropical Gyre. *Ecosystems*, *2*(3), 181–214. https://doi.org/10.1007/s100219900068

Kessler, W. S. (2006). The circulation of the eastern tropical Pacific: A review. *Progress in Oceanography*, *69*(2–4), 181–217. https://doi.org/10.1016/j.pocean.2006.03.009

Lee, D.-K., Niiler, P., Warn-Varnas, A., & Piacsek, S. (1994). Wind-driven secondary circulation in ocean mesoscale. *Journal of Marine Research*, *52*(3), 371–396.

Lorenzo, E. D., Schneider, N., Cobb, K. M., Franks, P. J. S., Chhak, K., Miller, A. J., McWilliams, J. C., Bograd, S. J., Arango, H., Curchitser, E., Powell, T. M., & Rivière, P. (2008). North Pacific Gyre Oscillation links ocean climate and ecosystem change. *Geophysical Research Letters*, *35*(L08607). https://doi.org/10.1029/2007GL032838

Marland, G., & Rotty, R. M. (1984). Carbon dioxide emissions from fossil fuels: A procedure for estimation and results for 1950-1982. *Tellus B: Chemical and Physical Meteorology*, *36*(4), 232–261. https://doi.org/10.3402/tellusb.v36i4.14907

McCreary, J. P., & Lu, P. (1994). Interaction between the subtropical and equatorial ocean circulations: The subtropical cell. *Journal of Physical Oceanography*, *24*(2), 466–497. https://doi.org/10.1175/1520-0485(1994)024<0466:IBTSAE>2.0.CO;2

McKinley, G. A., Fay, A. R., Takahashi, T., & Metzl, N. (2011). Convergence of atmospheric and North Atlantic carbon dioxide trends on multidecadal timescales. *Nature Geoscience*, *4*, 606–610. https://doi.org/10.1038/ngeo1193

McPhaden, M. J., & Zhang, D. (2002). Slowdown of the meridional overturning circulation in the upper Pacific Ocean. *Nature*, *415*(6872), 603–608. https://doi.org/10.1038/415603a

Pierrot, D., Neill, C., Sullivan, K., Castle, R., Wanninkhof, R., Lüger, H., Johannessen, T., Olsen, A., Feely, R. A., & Cosca, C. E. (2009). Recommendations for autonomous underway pCO2 measuring systems and data-reduction routines. *Deep Sea Research Part II: Topical Studies in Oceanography*, *56*(8–10), 512–522.

Pittman, N. A., Strutton, P. G., Johnson, R., Matear, R. J., & Sutton, A. J. (2022). Relationships between air-sea CO2 flux and new production in the equatorial Pacific. *Global Biogeochemical Cycles*, *36*(e2021GB007121). https://doi.org/10.1029/2021GB007121

Qui, S., Feng, Y., Zhang, Y., Qi, D., Wu, Y., & Du, Y. (2021). A surface pCO2 increasing hiatus in the equatorial Pacific Ocean since 2010. *Geophysical Research Letters*, *48*(21). https://doi.org/10.1029/2021GL093612

Rayner, P. J., & Law, R. M. (1999). The relationship between tropical CO2 fluxes and the El Niño-Southern Oscillation. *Geophysical Research Letters*, *26*(4), 493–496. https://doi.org/10.1029/1999GL900008

Rii, Y. M., Peoples, L. M., Karl, D. M., & Church, M. J. (2022). Seasonality and episodic variation in picoeukaryote diversity and structure reveal community resilience to

disturbances in the North Pacific Subtropical Gyre. *Limnology and Oceanography*, *67*, S331–S351.

Sabine, C. L., Feely, R. A., Gruber, N., Key, R. M., Lee, K., Bullister, J. L., Wanninkhof, R., Wong, C. S., Wallace, D. W. R., Tilbrook, B., Millero, F. J., Peng, T.-H., Kozyr, A., Ono, T., & Rios, A. F. (2004). The oceanic sink for anthropogenic CO2. *Science*, *305*, 367–371. https://doi.org/10.1126/science.1097403

Sarma, V. V. S. S., Saino, T., Sasaoka, K., Nojiri, Y., Ono, T., Ishii, M., Inoue, H. Y., & Matsumoto, K. (2006). Basin-scale pCO2 distribution using satellite sea surface temperature, Chl a, and climatological salinity in the North Pacific in spring and summer. *Global Biogeochemical Cycles*, *20*(GB3005). https://doi.org/10.1029/2005GB002594

Siegenthaler, U., & Wenk, T. (1984). Rapid atmospheric CO2 variations and ocean circulation. *Nature*, *308*, 624–626. https://doi.org/10.1038/308624a0

Sutton, A. J., Feely, R. A., Sabine, C. L., McPhaden, M. J., Takahashi, T., Chavez, F. P., Friedrich, G. E., & Jeremy T. Mathis. (2014). Natural variability and anthropogenic change in equatorial Pacific surface ocean pCO2 and pH. *Global Biogeochemical Cycles*, *28*(2), 131–145. https://doi.org/10.1002/2013GB004679

Sutton, A. J., Wanninkhof, R., Sabine, C. L., Feely, R. A., Cronin, M. F., & Weller, R. A. (2017). Variability and trends in surface seawater pCO2 and CO2 flux in the Pacific Ocean. *Geophysical Research Letters*, *44*(11), 5627–5636. https://doi.org/10.1002/2017GL073814

Swalwell, J. E., Ribalet, F., & Armbrust, V. E. (2011). SeaFlow: A novel underway flow-cytometer for continuous observations of phytoplankton in the ocean. *Limnology and Oceanography: Methods*, *9*(10), 466–477. https://doi.org/10.4319/lom.2011.9.466

Takahashi, T., Sutherland, S., & Kozyr, A. (2019). *Global Ocean Surface Water Partial Pressure of CO2 Database: Measurements Performed During 1957-2019* (LDEO Database Version 2019; 9.9) [Data set]. NOAA National Centers for Environmental Information; Carbon Dioxide Information and Analysis Center (CDIAC), Oak Ridge, National Laboratory. https://doi.org/10.3334/CDIAC/OTG.NDP088(V2015)

Takahashi, T., Sutherland, S., Wanninkhof, R., Sweeney, C., Feely, R., Chipman, D., Hales, B., Friedrich, G., Chavez, F., Sabine, C., Watson, A., Bakker, D., Schuster, U., Metzl, N., Yoshikawa-Inoue, H., Ishii, M., Midorikawa, T., Nojiri, Y., Körtzinger, A., … J.W. de Baar, H. (2009). Climatological mean and decadal change in surface ocean pCO2, and net sea–air CO2 flux over the global oceans. *Deep-Sea Research Part II: Topical Studies in Oceanography*, *56*(8–10), 554–577. https://doi.org/10.1016/j.dsr2.2008.12.009

Vaittinada Ayar, P., Bopp, L., Christian, J. R., Ilyina, T., Krasting, J. P., Séférian, R., Tsujino, H., Watanabe, M., Yool, A., & Tjiputra, J. (2022). Contrasting projections of the ENSO-driven CO2 flux variability in the equatorial Pacific under high-warming scenario. *Earth System Dynamics*, *13*, 1097–1118. https://doi.org/10.5194/esd-13-1097-2022

Wilson, C. (2003). Late summer chlorophyll blooms in the oligotrophic North Pacific Subtropical Gyre. *Geophysical Research Letters*, *30*(18), 1942. https://doi.org/10.1029/2003GL017770

Yasunaka, S., Kouketsu, S., Strutton, P. G., Sutton, A. J., Murata, A., Nakaoka, S., & Nojiri, Y. (2019). Spatio-temporal variability of surface water pCO2 and nutrients in the tropical Pacific from 1981 to 2015. *Deep-Sea Research Part II: Topical Studies in Oceanography*, *169–170*(November-December 2019, 104680). https://doi.org/10.1016/j.dsr2.2019.104680.